Comparing the Efficiency of DBS Patterns in a Stochastic Dynamical Model

Sofia D. Karamintziou[1], George L. Tsirogiannis[1], Pantelis G. Stathis[2], George A. Tagaris[2], Efstathios J. Boviatsis[2], Damianos E. Sakas[2] and Konstantina S. Nikita[1]

[1] Biomedical Simulations and Imaging Laboratory, National Technical University of Athens, 9 Iroon Polytechniou Str., 15780 Athens, Greece
[2]Department of Neurosurgery, University of Athens Medical School, "Evangelismos" General Hospital, 45–47 Ipsilantou Str., 10675 Athens, Greece
E-mails: skaram@biosim.ntua.gr and knikita@ece.ntua.gr

Abstract–A stochastic phase model is fitted to 216 microelectrode recordings (MERs), acquired during 18 surgical interventions in patients with Parkinson's disease (PD), in order to comparatively simulate the desynchronizing effect of regular (130 Hz) versus non-regular patterns of stimulation with the same mean frequency and increasing degrees of temporal variability. We demonstrate that non-regular patterns of stimulation displaying a minimum variability of 70-80% yield a significantly higher Lyapunov exponent compared with regular stimulation, at the 5% significance level. The stochastic model points to the prominent role of non-regular stimulation patterns in the therapeutic outcome of deep brain stimulation (DBS).

1. Introduction

Recent evidence signifies the potential importance of the temporal pattern of high frequency deep brain stimulation (DBS) in the clinical efficacy of this reference neurosurgical procedure [1, 2]. Temporally irregular DBS can suppress tremor if there are no long pauses [1], while it may ameliorate motor symptoms and suppress pathological rhythmic activity in Parkinson's disease (PD) more effectively than regular stimulation [2]. At the same time, alterations in the abnormal discharge pattern of subthalamic nucleus (STN) neurons [3] and disruption of neuronal synchronization [4-6] have been suggested to be involved in the therapeutic mechanisms of action of STN-DBS.

In this paper, we employ methods from stochastic nonlinear dynamics [7-9] to comparatively evaluate the Lyapunov exponent as a quantity reflecting subthalamic synchronization dynamics in response to regular (130 Hz) versus non-regular patterns of stimulation. A stochastic phase model is fitted to a total of 216 microelectrode recordings (MERs) corresponding to sites lying within the intraoperatively confirmed borders of the STN. The phase model is developed incorporating multiple factors affecting neuronal dynamics: neuronal coupling, intrinsic independent and extrinsic common noise sources, and external forcing. Non-regular patterns are generated by a gamma process with mean frequency of 130 Hz and increasing degrees of temporal variability [10].

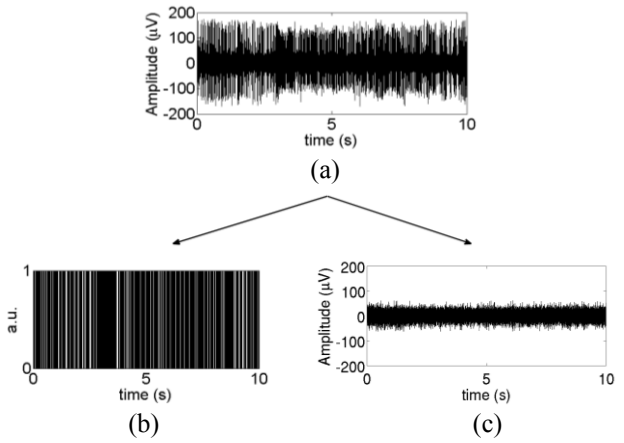

Figure 1: Two-scale neuronal activity (a) Example of raw extracellular signal recorded in the right STN, case 2 (recording site depth: A +0.5). (b)-(c) The two derived high-pass filtered signals: spiking activity (a.u.=arbitrary units) and background unit activity, respectively.

2. Patients and Methods

2.1. Patients and Surgery

During a 2-years period, 18 patients underwent bilateral implantation of DBS electrodes in the STN, at the Department of Neurosurgery, at Evangelismos General Hospital of Athens. The clinical criteria included idiopathic PD with motor fluctuations and/or dyskinesias. Stereotactic surgery was based on pre-operative anatomical targeting of the STN, MER and high frequency test stimulation [11].

2.2. Data Description-Signal Preprocessing

A commercially available microrecording system (Leadpoint TM Neural Activity Monitoring System, Medtronic Inc., Minneapolis, MN) is used to acquire and store data. In total, data from 72 MER trajectories are retrospectively analyzed in Matlab (Mathworks, Natick, MA). Initially, the acquired signals are digitally high-pass filtered at 0.5-10 kHz applying a 4-pole Butterworth filter. The method we present here is based on the assessment of

two-scale neuronal activity: a. spiking activity quantified through the spike detection process [12] and b. activity of small neural populations quantified through the background unit activity extraction process [13] (figure 1).

2.3. The Phase Model

We consider the following Langevin equation (by virtue of the Stratonovich interpretation [7]) describing an ensemble of N globally coupled identical phase oscillators, driven by intrinsic independent and extrinsic common noises, but also subject to external forcing:

$$\begin{aligned}\frac{\mathrm{d}\phi_i}{\mathrm{d}t} &= \omega + \frac{K}{N}\sum_{j=1}^{N}\sin\left(2\pi\left(\phi_j-\phi_i\right)\right)+\sigma_{\mathrm{I}}R_{\mathrm{I}}\left(\phi_i\right)\xi_i(t)\\ &+\sigma_{\mathrm{C}}R_{\mathrm{C}}\left(\phi_i\right)\eta(t)+\Delta\left(\phi_i,\beta\right)\sum_k\delta\left(t-\tau_k\right)\end{aligned} \tag{1}$$

Here, $\phi_i\in[0,1)$ is the phase variable of the *ith* oscillator, ω is its natural frequency and $K>0$ is the coupling strength. We assume that $\xi_i(t)$ is zero mean Gaussian white noise, added independently to each oscillator, with correlation specified by $\left\langle\xi_i(t)\xi_j(t')\right\rangle=\delta_{ij}\delta(t-t')$, where $\delta_{ij}=1$ if $i=j$ and 0 if $i\neq j$.We regard $\eta(t)$ as colored noise with zero mean and unitary variance, i.e. with autocorrelation function $C(t)=\langle\eta(t)\eta(0)\rangle=\frac{1}{2\tau_{\mathrm{C}}}e^{-\frac{|t|}{\tau_{\mathrm{C}}}}$. Thus, $\eta(t)$ can be regarded as an Ornstein-Uhlenbeck process with correlation time τ_{C} [7]. σ_{I} and σ_{C} are small parameters representing the intensity of independent and common noise, respectively. $R_{\mathrm{C}}\left(\phi_i\right)$ and $R_{\mathrm{I}}\left(\phi_i\right)$ are phase sensitivity functions that represent the linear response of the phase variable ϕ_i to the respective infinitesimal noise perturbations, while $\Delta\left(\phi_i,\beta\right)$ is the phase response curve (PRC) to a single (DBS) impulse [8, 9]. β represents the stimulus amplitude and τ_k are the input times. Introducing the Kuramoto order parameter defined by $re^{2\pi i\psi}=\frac{1}{N}\sum_{j=1}^{N}\mathrm{e}^{2\pi i\phi_j}$ [8], Eq. (1) can be rewritten as [14]:

$$\begin{aligned}\frac{\mathrm{d}\phi}{\mathrm{d}t} &= \omega+Kr\sin\left(2\pi\left(\psi-\phi\right)\right)+\sigma_{\mathrm{I}}R_{\mathrm{I}}\left(\phi\right)\xi(t)\\ &+\sigma_{\mathrm{C}}R_{\mathrm{C}}\left(\phi\right)\eta(t)+\Delta\left(\phi,\beta\right)\sum_k\delta\left(t-\tau_k\right)\end{aligned}, \tag{2}$$

where r characterizes the mean degree of synchrony and ψ is the mean phase of the oscillators. Next, defining the effective drift and diffusion coefficients [15]

$$v=\sigma_{\mathrm{C}}^2\int_0^\infty \mathrm{d}s C(s)\int_0^1 \mathrm{d}\phi R_{\mathrm{C}}'\left(\phi\right)R_{\mathrm{C}}\left(\phi-\omega s\right) \tag{3}$$

$$D=\sigma_{\mathrm{C}}^2\int_{-\infty}^\infty \mathrm{d}s C(s)\int_0^1 \mathrm{d}\phi R_{\mathrm{C}}\left(\phi\right)R_{\mathrm{C}}\left(\phi-\omega s\right) \tag{4}$$

we obtain the following white-noise Langevin equation:

$$\begin{aligned}\frac{\mathrm{d}\phi}{\mathrm{d}t} &= \omega+Kr\sin\left(2\pi\left(\psi-\phi\right)\right)+v+\left(\sigma_{\mathrm{I}}R_{\mathrm{I}}\left(\phi\right)+\sqrt{D}\right)\xi(t)\\ &+\Delta\left(\phi,\beta\right)\sum_k\delta\left(t-\tau_k\right)\end{aligned} \tag{5}$$

The Stratonovich Eq. (5) is converted to an equivalent Ito stochastic differential equation [7]:

$$\begin{aligned}\frac{\mathrm{d}\phi}{\mathrm{d}t} &= \omega+Kr\sin\left(2\pi\left(\psi-\phi\right)\right)+v+\left(\sigma_{\mathrm{I}}R_{\mathrm{I}}\left(\phi\right)+\sqrt{D}\right)\xi(t)\\ &+\frac{\sigma_{\mathrm{I}}}{2}R_{\mathrm{I}}'\left(\phi\right)\left(\sigma_{\mathrm{I}}R_{\mathrm{I}}\left(\phi\right)+\sqrt{D}\right)+\Delta\left(\phi,\beta\right)\sum_k\delta\left(t-\tau_k\right)\end{aligned} \tag{6}$$

Phase eq. (6) is solved through the stochastic map from one stimulus cycle to the next [16]. We consider that the inter-impulse interval (IPI) $\Delta\tau_n=\tau_{n+1}-\tau_n$ obeys the gamma distribution with a mean of 130Hz and increasing degrees of temporal variability [10]. The phase dynamics during the IPI $\Delta\tau_n$ is described by

$$\begin{aligned}\phi_{n+1} &= \phi_n\\ &+\left(\omega+Kr\sin\left(2\pi\left(\psi-\phi_n\right)\right)+v+\frac{\sigma_{\mathrm{I}}}{2}R_{\mathrm{I}}'\left(\phi_n\right)\right.\\ &\left.\times\left(\sigma_{\mathrm{I}}R_{\mathrm{I}}\left(\phi_n\right)+\sqrt{D}\right)\right)\Delta\tau_n+\left(\sigma_{\mathrm{I}}R_{\mathrm{I}}\left(\phi_n\right)+\sqrt{D}\right)W\left(\Delta\tau_n\right)\\ &+\Delta\left(\phi_n,\beta\right)\end{aligned} \tag{7}$$

where $W(t)$ is a Wiener process with probability density function (PDF) f_{W_t}, which is a Gaussian with zero mean and variance $\Delta\tau$. The stochastic map is defined by the Perron-Frobenius operator, that maps the density of phases at the time of the $(n+1)th$ impulse, $p_{n+1}(\phi)$, onto the density of phases at the time of the *nth* impulse, $p_n(\phi)$ [17,18,19]:

$$\begin{aligned}p_{n+1}(\phi) &= \\ &\int_0^1\int_0^\infty \mathrm{d}(\Delta\tau)\sum_{j\in Z}f_{W_t}\left(\frac{\phi-\phi'+j}{\left(\sigma_{\mathrm{I}}R_{\mathrm{I}}(\phi')+\sqrt{D}\right)}\right.\\ &-\frac{\left(\omega+Kr\sin\left(2\pi\left(\psi-\phi'\right)\right)+v+\frac{\sigma_{\mathrm{I}}}{2}R_{\mathrm{I}}'(\phi')\left(\sigma_{\mathrm{I}}R_{\mathrm{I}}(\phi')+\sqrt{D}\right)\right)}{\left(\sigma_{\mathrm{I}}R_{\mathrm{I}}(\phi')+\sqrt{D}\right)}\\ &\left.\times\Delta\tau-\frac{\Delta(\phi',\beta)}{\left(\sigma_{\mathrm{I}}R_{\mathrm{I}}(\phi')+\sqrt{D}\right)}\right)\times G(\Delta\tau)\\ &\times\frac{1}{\left(\sigma_{\mathrm{I}}R_{\mathrm{I}}(\phi')+\sqrt{D}\right)}p_n(\phi')\mathrm{d}\phi'\end{aligned} \tag{8}$$

where $G(\Delta\tau)$ is the PDF of the IPIs. Discretizing the density into $M=500$ bins of size $1/M$, the stochastic map is approximated using a 500×500 transition matrix $A(\phi,\phi')$ (stochastic kernel) having all positive entries and a spectral radius of 1 [17, 18] (figure 2). This matrix possesses the strong Perron-Frobenius property [20]. The iterated mapping (8) converges to the steady-state phase distribution (invariant density), $p_{\mathrm{st}}(\phi)$, represented by the eigenvector corresponding to the dominant (unit) eigenvalue of the transition matrix. To quantify the stability of the synchronized states we calculate the Lyapunov exponent, using phase map (7), as [21, 22]:

$$\lambda = \frac{\left\langle \ln\left|\mathrm{d}\phi_{n+1} / \mathrm{d}\phi_n\right|\right\rangle}{\left\langle \Delta\tau \right\rangle} = \frac{1}{\left\langle \Delta\tau \right\rangle}\int_0^1 \mathrm{d}\phi \int_0^\infty \mathrm{d}(\Delta\tau)\times$$
$$\ln\left|1 + \left(-2\pi Kr\cos(2\pi(\psi-\phi))\right.\right.$$
$$\left.\left. + \frac{\sigma_\mathrm{I}}{2} R_\mathrm{I}''(\phi)\left(\sigma_I R_\mathrm{I}(\phi) + \sqrt{D}\right)\right)\Delta\tau\right.$$
$$\left. + \Delta'(\phi,\beta)\right| \cdot p_{\mathrm{st}}(\phi) \qquad (9)$$

where $\left\langle \Delta\tau \right\rangle^{-1} = 130\mathrm{Hz}$. Nonpositive values of the Lyapunov exponent indicate synchronization.

2.4. Determination of Phase Sensitivity Functions

Taking into consideration that for weak Gaussian common driving noise, a Type-II PRC is optimal for stochastic synchronization [23], we use this shape for the phase sensitivity to common noise in order to simulate the state of pathological synchronization in PD. A Type-I PRC is selected for the phase sensitivity to independent noise. Accordingly we consider

$$R_\mathrm{C}(\phi) = \sqrt{2}\left(-\sin(2\pi\phi)\right) \text{ and } R_\mathrm{I}(\phi) = \sqrt{\frac{2}{3}}\left(1-\cos(2\pi\phi)\right)$$

Differently, there is evidence that the type 0 PRC may be optimal for stochastic desynchronization [24]. Hence, in order to simulate the desynchronizing effect of DBS we consider $\Delta(\phi,0) = 0$ and

$$\Delta(\phi,\beta) = \begin{cases} \phi\, \mathrm{e}^{(10-\beta)(\phi-0.5)} & 0 \le \phi \le 0.5 \\ (\phi-1)\mathrm{e}^{-(10-\beta)(\phi-0.5)} & 0.5 \le \phi < 1 \end{cases}, \qquad (10)$$

where $0 < \beta \le 5$.

2.5. Determination of Model Parameters

There are eight parameters that must be estimated in the phase model (6): ω , r , K , ψ , σ_C , v , D and σ_I . We set $\omega = 1$ according to [6]. The modulus r of the order parameter (mean degree of synchrony) and the coupling strength K are adjusted to effect a substantial neural correlation but not perfect synchrony in the absence of stimulation [6]. Hence, we set $K = 0.8$ and $r = 0.44$ .We also consider $\psi = 0$. As indicated by Eqs. (3) and (4) calculation of parameters v and D is dependent on estimation of σ_C and $C(t)$. The intensity of common noise σ_C is determined through evaluation of the power spectral density function of the background unit activity [13] using Welch's method, while the autocorrelation function of the same signal is used as an estimate of $C(t)$.

We proceed to evaluate the intensity of the independent noise σ_I , through definition of the first passage time problem for the phase model (6) with no input. Let $\rho(\phi,t)$ represent the PDF of phases at time t .The corresponding Fokker-Planck equation is [7]

$$\frac{\partial\rho}{\partial t} = -\frac{\partial}{\partial\phi}\left\{\left[\omega + Kr\sin(2\pi(\psi-\varphi)) + v + \frac{\sigma_\mathrm{I}}{2}R_\mathrm{I}'(\phi)\right.\right.$$
$$\left.\left.\times\left(\sigma_\mathrm{I}R_\mathrm{I}(\phi) + \sqrt{D}\right)\right]\rho\right\} + \frac{1}{2}\frac{\partial^2}{\partial\phi^2}\left\{\left(\sigma_\mathrm{I}R_\mathrm{I}(\phi) + \sqrt{D}\right)^2\rho\right\} \qquad (11)$$

with periodic boundary condition $\rho(0,t) = \rho(1,t)$. Extending the definition of the phase from $\phi \in [0,1)$ to $\phi \in \Re$ and considering $\sigma_\mathrm{I} \ll 1$, we obtain the following approximations [25]:

$R_\mathrm{I}(\phi) \approx R_\mathrm{I}(t)$ and $Kr\sin(2\pi(\psi-\phi)) \approx Kr\sin(2\pi(\psi-t))$. The Fokker-Planck equation for the corresponding PDF $\zeta(\phi,t)$ is

$$\frac{\partial\zeta}{\partial t} = -\left[\omega + Kr\sin(2\pi(\psi\text{-}t)) + v + \frac{\sigma_\mathrm{I}}{2}R_I'(t)\right.$$
$$\left.\times\left(\sigma_\mathrm{I}R_\mathrm{I}(t) + \sqrt{D}\right)\right]\frac{\partial\zeta}{\partial\phi} + \frac{\left(\sigma_\mathrm{I}R_\mathrm{I}(t) + \sqrt{D}\right)^2}{2}\frac{\partial^2\zeta}{\partial\phi^2} \qquad (12)$$
$$\zeta(\phi,0) = \delta(\phi) \ , \ \phi \in \Re .$$

By taking the inverse Fourier Transform of $\tilde{\zeta}(\eta,t) = \int_{\Re} \mathrm{e}^{-i\eta\phi}\zeta(\phi,t)\mathrm{d}\phi$, with $\tilde{\zeta}(\eta,0) = 1$, we obtain:

$$\zeta(\phi,t) = \frac{1}{\left(2\pi\left(\sigma_\mathrm{I}{}^2\int_0^t R_\mathrm{I}^2(s)ds + 2\sigma_\mathrm{I}\sqrt{D}\int_0^t R_\mathrm{I}(s)ds + Dt\right)\right)^{1/2}}$$
$$\times\exp\left(-\frac{\left((\omega+v)t + \frac{1}{2\pi}Kr\cos(2\pi(\psi-t)) - \phi\right.}{2\left(\sigma_\mathrm{I}^2\int_0^t R_\mathrm{I}^2(s)ds + 2\sigma_\mathrm{I}\sqrt{D}\int_0^t R_\mathrm{I}(s)ds + Dt\right)}\right.$$
$$\left.\left. + \frac{\sigma_\mathrm{I}^2}{4}R_\mathrm{I}^2(t) + \frac{\sigma_I\sqrt{D}}{2}R_\mathrm{I}(t)\right)^2$$
$$\left.\frac{}{2\left(\sigma_\mathrm{I}^2\int_0^t R_\mathrm{I}^2(s)ds + 2\sigma_\mathrm{I}\sqrt{D}\int_0^t R_\mathrm{I}(s)ds + Dt\right)}\right) \qquad (13)$$

Respectively, the first passage time distribution is simply $z(t) = \zeta(1,t)$. Finally, maximization of the log likelihood function L over σ_I yields an estimate for σ_I [16]:

$$\frac{\mathrm{d}}{\mathrm{d}\sigma_\mathrm{I}}L\left(\sigma_\mathrm{I}\middle|\{\Delta t_i\},v,D\right) = \frac{\mathrm{d}}{\mathrm{d}\sigma_\mathrm{I}}\sum_i \ln z\left(\Delta t_i\middle|\sigma_\mathrm{I},v,D\right) = 0 \qquad (14)$$

where $\{\Delta t_i\}$ are the interspike interval (ISI) data.

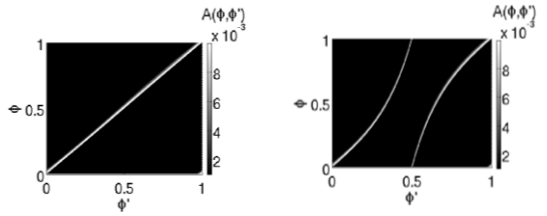

(a) (b)

Figure 2: Stochastic kernel functions based on MER at C 0, right STN, case 1, (a) for $\beta = 0$ and (b) for $\beta = 5$, and pattern variability of 70%.

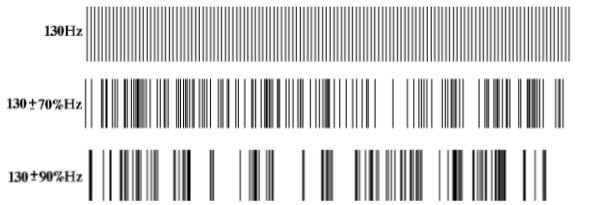

(a)

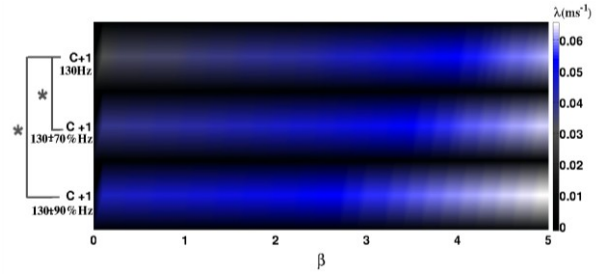

(b)

Figure 3: Simulation results. (a) Application of three distinct stimulation patterns and (b) the respective Lyapunov exponent λ as a function of the stimulus amplitude β, at site C +1, right STN, case 14. Asterisks denote significant differences ($p < 0.05$).

3. Results

Figure 2 depicts the stochastic kernel functions for two values of stimulus amplitude β and pattern variability of 70%, derived based on MER at a specific site depth. For $\beta = 0$, the proposed phase model reproduces the pathological synchronized state ($\phi = \phi'$), while for $\beta = 5$, the obtained state is less synchronized. Figure 3(b) displays the Lyapunov exponent for three distinct stimulation patterns, as a function of stimulus amplitude, derived based on the analysis of MER at a particular site depth. Overall, the Lyapunov exponent gradually increases with increasing stimulus amplitude, thereby reflecting the ability of the model to simulate the desynchronizing effect of stimulation [3-6]. Importantly, values of the Lyapunov exponent corresponding to each of the irregular patterns of stimulation are significantly higher than the values of the exponent corresponding to the regular pattern of stimulation ($p < 0.05$). In the total of the recordings examined, this significant difference was verified for stimulation patterns displaying a minimum temporal variability of 70-80%.

4. Conclusion

Application of the proposed stochastic dynamical model to data pertinent to physiologically-guided DBS procedures signified the role of alternative stimulation patterns characterized by temporal irregularity in a potentially more effective symptom control in PD. Additional effect evaluation of long pauses and bursts in temporally irregular stimulation patterns [1, 2] would provide a deeper insight into the specific stimulation characteristics correlated with improved efficacy in PD.

References

[1] M. J. Birdno, A. M. Kuncel, A. D. Dorval, D. A.Turner, R. E. Gross, and W. M. Grill, J. Neurophysiol. **107**, 364 (2012).

[2] D. T. Brocker, B. D. Swan, D. A. Turner, R. E. Gross, S. B. Tatter, M. Miller Koop, H. Bronte-Stewart, and W. M. Grill, Exp. Neurol. **239**, 60 (2013).

[3] J. D. Carlson, D. R. Cleary, J. S. Cetas, M. M. Heinricher, and K. J. Burchiel, J. Neurophysiol. **103**, 962 (2010).

[4] C. Hauptmann, O. Popovych, and P. A. Tass, Expert Rev. Med. Devices **4**, 633 (2007).

[5] J. Modolo and A. Beuter, Med. Eng. Phys. **31**, 615 (2009).

[6] C. J. Wilson, B. 2nd Beverlin, and T. Netoff, Neurosci. **5**, 1 (2011).

[7] C. Gardiner, *Handbook of Stochastic Methods* (Berlin: Springer, 1985).

[8] Y. Kuramoto, *Chemical Oscillations, Waves, and Turbulence* (New York: Springer, 1984).

[9] A. T. Winfree, *The Geometry of Biological Time* (New York: Springer, 2001).

[10] A. D. Dorval, A. M. Kuncel, M. J. Birdno, D. A. Turner, and W. M. Grill, J. Neurophysiol. **104**, 911 (2010).

[11] D. E. Sakas, A. T. Kouyialis, E. J. Boviatsis, I. G.. Panourias, P. Stathis, and G. Tagaris, Acta Neurochir. Suppl. **97**, 163 (2007).

[12] S. Wong, G. H. Baltuch, J. L. Jaggi, and S. F. Danish, J. Neural Eng. **6,** 1 (2009).

[13] A. Moran and I. Bar-Gad, J. Neurosci. Methods **186,** 116 (2010).

[14] S. H. Strogatz, Physica D **143**, 1 (2000).

[15] H. Nakao, J. Teramae, D. Goldobin, and Y. Kuramoto, Chaos **20,** 033126 (2010).

[16] W. H. Nesse and G. A. Clark, Biol. Cybern. **102**, 389 (2010).

[17] B. Ermentrout and D. Saunders, J. Comput. Neurosci. **20,** 179 (2006).

[18] T. Yamanobe and K. Pakdaman, Biol. Cybern. **86,** 155, (2002).

[19] S. Hata, T. Shimokawa, K. S. Arai, and H. Nakao, Phys. Rev. E **82**, 036206 (2010).

[20] D. Noutsos and M. Tsatsomeros, SIAM J. Matrix Anal. & Appl. **30,** 700 (2008).

[21] A. Pikovsky, M. G. Rosenblum, and J. Kurths, *Synchronization: A Universal Concept in Nonlinear Sciences* (Cambridge University Press, 2001).

[22] J. N. Teramae and D. Tanaka, Phys. Rev. Lett. **93**, 204103 (2004).

[23] A. Abouzeid and B. Ermentrout, Phys. Rev. E **80,** 011911 (2009).

[24] S. Hata, K. Arai, R. F. Galán, and H. Nakao, Phys. Rev. E **84**, 016229 (2011).

[25] C. Ly and G. B. Ermentrout, Physica D **240,** 719 (2011).